Science of the Total Environment 858 (2023) 159412

Contents lists available at ScienceDirect

Science of the Total Environment

journal homepage: www.elsevier.com/locate/scitotenv

A mechanistic approach to include climate change and unplanned urban sprawl in landslide susceptibility maps

Elisa Bozzolan [a,d,e,*], Elizabeth A. Holcombe [a,d], Francesca Pianosi [a,d], Ivan Marchesini [b], Massimiliano Alvioli [b], Thorsten Wagener [a,c,d]

[a] Department of Civil Engineering, University of Bristol, Bristol BS8 1SS, UK
[b] Consiglio Nazionale delle Ricerche, Istituto di Ricerca per la Protezione Idrogeologica, via Madonna Alta 126, I-06128 Perugia, Italy
[c] Institute of Environmental Science and Geography, University of Potsdam, Potsdam, Germany
[d] Cabot Institute, University of Bristol, Bristol, UK
[e] Department of Geosciences, University of Padua, Via Giovanni Gradenigo, 6, 35131 Padova (PD), Italy

HIGHLIGHTS

- Urban and climatic changes have not yet been considered jointly in regional landslide susceptibility assessments.
- We present a methodology based on repeated simulations of a mechanistic model to account for these environmental changes
- Unplanned urban sprawl can be more detrimental than climate change for slope stability; their joint impact is greater than the sum of its parts.
- Our regional susceptibility maps can be updated with new data, projections and planning strategies

GRAPHICAL ABSTRACT

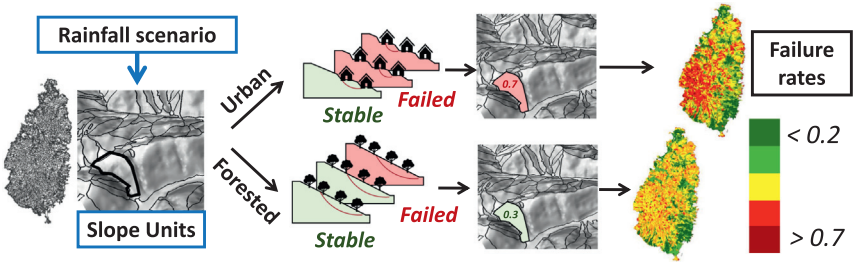

ARTICLE INFO

Editor: Fernando A.L. Pacheco

Keywords:
Landslide susceptibility
Informal housing
Climate change
Humid tropics
Data paucity
Uncertainty
Global sensitivity analysis

ABSTRACT

Empirical evidence shows that climate, deforestation and informal housing (i.e. unregulated construction practices typical of fast-growing developing countries) can increase landslide occurrence. However, these environmental changes have not been considered jointly and in a dynamic way in regional or national landslide susceptibility assessments. This gap might be due to a lack of models that can represent large areas (>100km^2) in a computationally efficient way, while simultaneously considering the effect of rainfall infiltration, vegetation and housing. We therefore suggest a new method that uses a hillslope-scale mechanistic model to generate regional susceptibility maps under changing climate and informal urbanisation, which also accounts for existing uncertainties. An application in the Caribbean shows that the landslide susceptibility estimated with the new method and associated with a past rainfall-intensive hurricane identifies ~67.5 % of the landslides observed after that event. We subsequently demonstrate that the hypothetical expansion of informal housing (including deforestation) increases landslide susceptibility more (+20 %) than intensified rainstorms due to climate change (+6 %). However, their combined effect leads to a much greater landslide occurrence (up to +40 %) than if the two drivers were considered independently. Results demonstrate the importance of including both land cover and climate change in landslide susceptibility assessments. Furthermore, by modelling mechanistically the overlooked dynamics between urban growth and climate change, our methodology can provide quantitative information of the main landslide drivers (e.g. quantifying the relative impact of deforestation vs informal urbanisation) and locations where these drivers are or might become most detrimental for

* Corresponding author at: University of Bristol, Bristol, UK; University of Padua; Cabot Institute
E-mail addresses: elisa.bozzolan@bristol.ac.uk (E. Bozzolan), Liz.Holcombe@bristol.ac.uk (E.A. Holcombe), Francesca.Pianosi@bristol.ac.uk (F. Pianosi), ivan.marchesini@irpi.cnr.it (I. Marchesini), massimiliano.alvioli@irpi.cnr.it (M. Alvioli), thorsten.wagener@uni-potsdam.de (T. Wagener).

http://dx.doi.org/10.1016/j.scitotenv.2022.159412
Received 13 July 2022; Received in revised form 29 September 2022; Accepted 9 October 2022
Available online 13 October 2022

slope stability. Such information is often missing in data-scarce developing countries but is key for supporting national long-term environmental planning, for targeting financial efforts, as well as for fostering national or international investments for landslide mitigation.

1. Introduction

Worldwide empirical evidence shows that landslide incidence can increase under expanding deforestation (Glade, 2003; Pisano et al., 2017; Reichenbach et al., 2014), informal housing (i.e. housing that does not conform with building regulations such as unregulated hill cutting or unmanaged water drainage - Anderson et al., 2008; Diaz, 1992; Smyth and Royle, 2000) and changing precipitation patterns (Haque et al., 2019; Gariano et al., 2015). These environmental changes should therefore be included in landslide predictions, especially in the Tropics where informal urban population is rapidly expanding (Ozturk et al., 2022) and rainfall events can be very intense (Seneviratne et al., 2012). However, current methods to quantify landslide susceptibility (which identifies where hillslopes are more prone to failure) are not adequate in fast changing environments, as they fail to capture the dynamic effects of changing climate and expanding urbanisation, and do not consider the potentially large uncertainties in these landslide drivers, underlying slope or soil characteristics. Amongst these methods, the most employed use statistical and mechanistic slope stability models.

Statistical models are typically used to derive landslide susceptibility maps at national and regional (>100km^2) scales. These models employ data available at these scales (such as Digital Elevation Models - DEM) to derive their correlation with historical landslides: more failures are predicted to occur in locations similar to those where they happened before (see Reichenbach et al., 2018 for a review on the topic). Unfortunately, this approach is inapplicable in places where (1) landslide records are missing or unreliable (as in many landslide-prone tropical countries - Maes et al., 2017), (2) urbanisation is growing fast, and thus landscape properties are changing (UN, 2019); (3) decision makers want to consider environmental conditions yet unseen, such as unprecedented extreme rainfall events due to climate change.

Spatially distributed mechanistic slope stability models rely less on landslides records because they parameterize causal relationships rather than correlations in historical data. As a consequence, they can be used to predict the effects of future, unseen environmental conditions. Nonetheless, these models have mostly been applied in small areas (<5–20 km^2), and almost always treating land cover and climate change separately (e.g., Van Beek and Van Asch, 2004; Vanacker et al., 2003; Melchiorre and Frattini, 2012). Only recently, efforts have been made to fill this gap. For example, Alvioli et al. (2018) explored the impact of a future climate scenario on landslide occurrence over an area of 420 km^2 in Central Italy. In their analysis, all geotechnical and hydrological parameters were fixed at 'worst case' values to better detect the impact of climate change on landslide occurrence. Bernardie et al. (2020) and Hürlimann et al. (2022) quantified the changes in regional landslide susceptibility under both vegetation and climate change scenarios for the French (70 km^2) and Spanish (326 km^2) Central Pyrenees respectively, while considering the uncertainty of some soil parameters. Although these studies are interesting in the spatial extent they have been able to tackle, they still only consider a limited number of possible climate/land cover scenarios and uncertain input data (the variation of which could lead to significantly different slope stability results, Melchiorre and Frattini, 2012) – probably due to the high computational running time of these models. Furthermore, none of these studies included the impacts of informal urban activities that are known to be detrimental for slope susceptibility, such as slope cutting or leaking pipes (e.g., Larsen, 2008; Anderson and Holcombe, 2013).

In this paper, we therefore suggest a new method that smartly uses a fast hillslope-scale mechanistic model to generate regional susceptibility maps under a wide range of climate change and - for the first time – informal urban expansion scenarios. In a previous study (Bozzolan et al., 2020), we have shown that the joint effect of different climate and localised urban construction activities can lead to significantly different slope stability responses. We did this by using a mechanistic model that can represent dynamic hydrological changes due to changes in climate (rainfall), vegetation and localised urban construction activities. Furthermore, as the model is fast to run, it could be applied within a Monte-Carlo (MC) simulation framework to account for uncertainty in the rainfall and urban drivers as well as in all hillslope properties and water table levels.

Here, we take that approach to the next level. Through Monte Carlo simulations, we generated a large library of synthetic hillslopes representative of the study area (the Caribbean island of Saint Lucia) and we analysed their stability under a wide range of different rainfall, vegetation and urban conditions. Differently from Bozzolan et al. (2020), we sampled the hillslope's geometric, geotechnical and soil properties to represent the variability of slopes across a region (the island of Saint Lucia) instead of the uncertainty about one specific location. By creating a sufficiently large catalogue of model runs, we could then map back the landslide predictions across that region, and so produce landslide susceptibility maps for many different storm events and land cover scenarios. For this work, we first tested the new method against observed landslides and we then created new susceptibility maps under hypothetical land cover and climate change scenarios. The research questions we aimed to answer are:

1) Which are the model's input factors that dominate the slope stability response at regional scale, whose uncertainty most affect our landslide susceptibility assessment?
2) How well can our landslide susceptibility map built under the scenario of a known rainfall event represent the landslides observed after that event?
3) How does current landslide susceptibility change under hypothetical scenarios of unregulated housing, deforestation and climate? How does the joint impact of these environmental drivers affect landslide susceptibility predictions?

The suggested approach is capable of dealing with non-stationary conditions (as suggested by Gariano and Guzzetti, 2016; and van Westen et al., 2006) and it can be updated as soon as new information (e.g. climate projections or urban plans) become available, just by selecting the most relevant modelled scenario. This is not possible for other methods such as statistically-based models, where the functional relationship between landscape attributes and past landslides might not hold under changed environmental conditions and new output maps must be re-calculated when new information becomes available (Reichenbach et al., 2018). Furthermore, the results presented are unique as they include for the first time both informal housing and climate change in regional landslide susceptibility assessments. We show that the comparison between scenarios allows the quantification of the relative and joint impact of rainfall and urban drivers on landslide predictions. Such quantitative information is often missing in developing, data-scarce nations but is key for policy decision makers to prioritise funding in urban planning and landslide mitigation actions (e.g. reforestation vs urban regulation) as well as for increasing awareness on the relative impact of different environmental changes.

2. The case study: Saint Lucia, Eastern Caribbean

Saint Lucia is an Eastern Caribbean island (617 km^2) with a humid tropical climate. The main landslide trigger is rainfall, and shallow rotational landslides dominate on both steep and shallow slopes (Anderson and

Holcombe, 2013; Migoń, 2010). The geology is almost entirely comprised of volcanic bedrock and deep volcanic deposits. Due to the climate, these volcanic parent materials are subjected to deep weathering, which decreases their strength and increases landslide susceptibility. The strata of a typical slope cross section comprise weathered residual soils and colluvium overlying decomposed rock and volcanic bedrock. These three types of strata typically correspond, respectively, to the weathering grades V–VI, III–IV, and I–II of the Hong Kong Geotechnical Engineering Office weathering grade classification (GEO, 1988). The textural composition and geotechnical characteristics of the upper soil strata are highly variable, but they can broadly be classified as fine-grained soils such as silty clays, clayey silts, and sandy clays (DeGraff, 1985). The combination of tropical climate, steep topography, and volcanic geology renders the region particularly susceptible to rainfall-triggered landslides. Furthermore, landslide risk is increased by informal housing which occupies steep slopes and employs unregulated engineering practices (World Bank, 2012; p. 226–235).

3. Method

This section describes the method used to generate ensembles of susceptibility maps of Saint Lucia under changing rainfall and/or urban expansion scenarios. We first generated a library of synthetic 2D cross-sectional hillslopes, whose properties are representative of the study area. Then, we analysed their stability response with a hillslope-scale mechanistic model (here the Combined Hydrology And Stability Model, CHASM) under different land covers and rainfall conditions. Finally, we linked these 2D synthetic hillslopes to 3D slope units – SUs (i.e. mapping units bounded by drainage and divide lines - Carrara et al., 1991; Guzzetti et al., 1999; Carrara et al., 1995), assigning to the SUs the stability response that corresponded to the rainstorm and land cover scenarios of interest.

Specifically, the methodological workflow (Fig. 1) develops in the following steps:

1. We identified the main land covers from available maps and subdivided the study area into SUs using a Digital Elevation Model (DEM). Each SU was defined by summary measures describing the variability of its height and slope gradient (e.g. the mean of the pixels' gradients). In this analysis, four land covers were considered: forest, shrub, bare and urban.
2. We defined the probability distributions of the input factors. In this context, the input factors represent all the input data needed to define the synthetic hillslopes within CHASM. This data includes the hillslope cross-sectional geometry (extrapolated from the SUs properties defined in the previous step) as well as the soil, urban and rainfall properties. The probability distributions aim to represent both the variability and the uncertainty of these properties across Saint Lucia and were defined based on a combination of: information available in the literature, data collected from the field in collaboration with local experts (critically including previous studies within informal communities which provided information on soil strata depths, cut slope angles, and other type of urban construction practices), or to best represent our lack of knowledge (e.g., using uniform distributions). Definitions of the probability distributions and their parameters are given in Section 3.2 and supplementary material.
3. We employed a statistical approach to randomly sample different values of input factors from their probability distributions. This process generated thousands of combinations of input factors, each one defining a possible synthetic hillslope in Saint Lucia. The sampling was carried out for the four main land cover types (bare, urban, forest, shrub) identified in step 1, thus generating four libraries of synthetic hillslopes. The stability of each hillslope was assessed with respect to a selected rainfall event (such as Hurricane Tomas) with CHASM (able to represent dynamic rainfall infiltration) and categorised according to the resulting minimum factor of safety (*FoS*): stable if $FoS \geq 1$, unstable otherwise.
4. We applied Global Sensitivity Analysis (Saltelli et al., 2008) to the dataset generated in step 3, in order to identify the input factors, including rainfall intensity and duration, that mostly control the CHASM's slope stability response. We defined these factors as 'dominant'. Determining dominant factors is important to reduce the complexity of the next step, where we will link the synthetic hillslopes in our libraries to the Slope Units (SUs) in our study area.
5. Using various data sources (DEM, land cover maps, etc.), we assigned the dominant factors (e.g. a slope angle value – step 5 in Fig. 1) to each SU. We could then associate each SU with those CHASM's simulations that have sufficiently 'similar' values of the dominant factors (e.g. a slope angle $\pm 5°$). Note that multiple synthetic slopes are linked to the same SU, as in building the libraries (step 3) we sampled the input variability space very densely (for example in the Results presented later, we had about 6500 SUs and generated 30,000 synthetic slopes for each land cover type). Once this linking was established, we could retrieve those linked synthetic hillslopes forced by the rainfall intensity-duration combination of interest (or sufficiently similar). We then calculated the percentage of these slopes that were predicted to fail: this value (failure rate, FR) will be displayed in the susceptibility map as the measure of failure frequency of that SU under the chosen rainstorm conditions (step 7–8 in Fig. 1). Similarly, we could generate susceptibility maps for different land cover scenarios by choosing the linked synthetic hillslopes from the library corresponding to the new land cover (e.g. from forest to bare, if we want to assess the impact of deforestation), and updating the failure rate accordingly.

In the next sections, we describe each methodological step represented in Fig. 1 more in detail.

3.1. Identify the main land cover and subdivide the study area into Slope Units

The main land covers in Saint Lucia were identified using a land cover map from 2015. This map was prepared by the British Geological Survey applying object-oriented image classification of satellite images (Jetten, 2016). From the original map, we merged the classes representing deep-rooted vegetation (e.g., mixed and lowland forest) into a single 'forest' class, and all shallow-rooted (e.g., shrubland and herbaceous agriculture) vegetation into a single 'shrub' class. The class 'urban' encompasses both buildings and roads. Fig. 2A shows the resulting land cover map used for this work, with the main three land cover classes considered: forest, shrub, urban. We also considered the land cover bare (which is present but not dominant) to allow comparison between the stability of non-urbanised bare slopes and vegetated slopes.

To automatically delineate SUs, we employed the open source r.slopeunits software (Alvioli et al., 2016) and the optimization strategy of Alvioli et al. (2020, 2022). We used a 5 m resolution DEM obtained from contour lines, derived from a national topographic map using photogrammetric methods in 2009–2010 (before the hurricane Tomas). Due to tropical vegetation and cloud cover the number of photogrammetric points was however often not sufficient to generate accurate contour lines in forested and cloud covered areas. The resulting DEM thus does not accurately represent the terrain situation in many locations (as shown in Fig. 5-2 in van Westen, 2016).

Fig. 2B shows the resulting SUs map. Details about execution of r.slopeunits software in the study area are reported in the supplementary material accompanying this paper, Section 1. The map contains 6496 Slope Units. Each SU is a polygon with size and shape dictated by local drainage setting, as captured from the DEM by the software r.slopeunits.

3.2. Definition of the variability range of input factors

The method involves the generation of synthetic hillslopes representative of Saint Lucia. The stability of these hillslopes was evaluated with CHASM, a model that requires information on hillslope geometry (e.g. slope angle, slope height and slope material strata), soil (geotechnical and hydrological), rainfall (i.e. intensity and duration) and initial boundary conditions (e.g. initial water depth) of 2D cross-sectional hillslopes. These

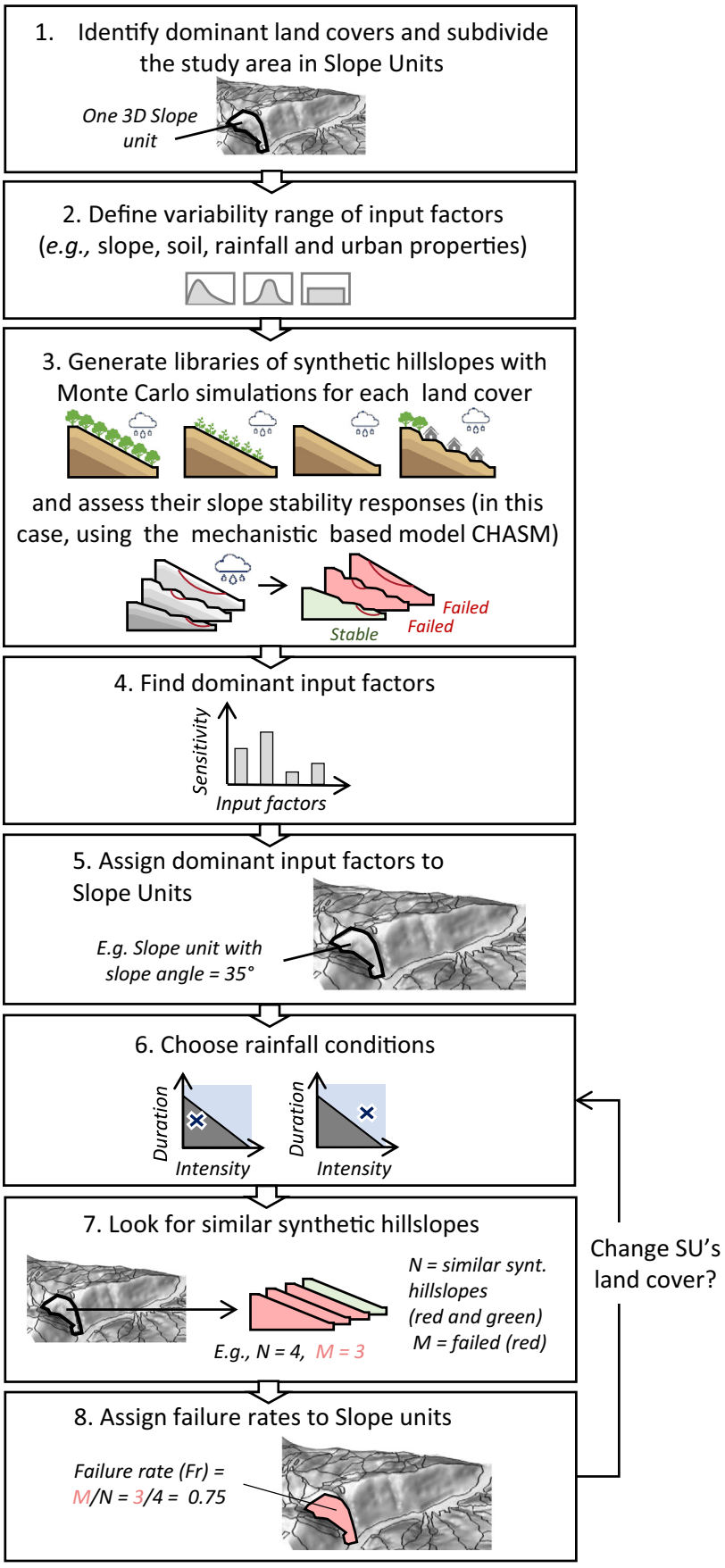

Fig. 1. Flowchart of the proposed method.

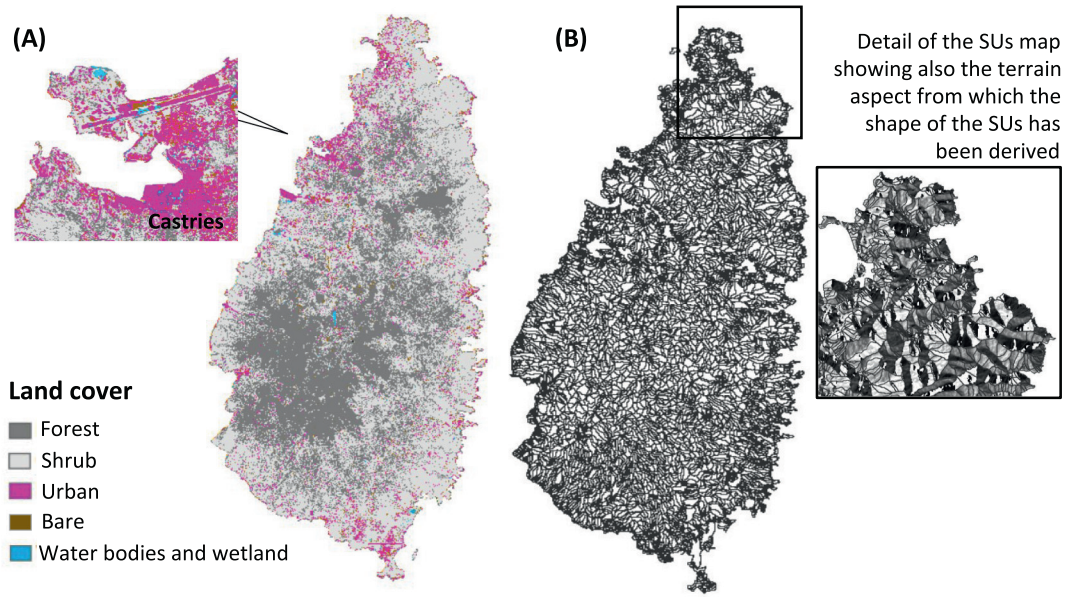

Fig. 2. (A) Land cover map where different land cover types have been grouped into 5 classes: forest, shrub, bare, urban and water bodies (original version: *http://www.charim.net/stlucia/maps*). (B) Slope Units (SUs) across Saint Lucia. On the right-hand side, a zoom-in of the map, showing the SUs overlaying the terrain aspect (derived from the DEM, available at http://www.charim-geonode.net/layers/geonode:dem).

Table 1
Varying input factors and their probability distributions.

Input factors	Symbol/Unit	Variability range			
Slope geometric properties:			Layer 1 *	Layer 2 *	Layer 3 *
Slope angle	δ [degrees]	U (5, 70)			
Slope height	H [m]	U (5, 100)			
Thickness of layer	H1 – H2 [m]		U (1,6)	U (1,6)	
Soil properties:					
Effective cohesion [a]	c [kPa]		Ln (2.368, 0.569)	Ln (3.4121, 0.577)	80
Effective friction angle [b]	φ [degrees]		Ln (3.293, 0.209)	Ln (3.1559, 0.325)	60
Dry unit weight [c]	γd [kN m^{-3}]		U (16,18)	U (18, 20)	23
Saturated moisture content [d]	VG θsat [m^3 m^{-3}]		N (0.413, 0.074)	N (0.413, 0.074)	N (0.413, 0.074)
Residual moisture content [d]	VG θres [m^3 m^{-3}]		Ln (−1.974, 0.376)	Ln (−1.974, 0.376)	Ln (−1.974, 0.376)
VG alpha parameter [d]	VG α [m^{-1}]		Ln (1.264, 1.076)	Ln (1.264, 1.076)	Ln (1.264, 1.076)
VG n parameters [d]	VG n		Ln (0.364, 0.358)	Ln (0.364, 0.358)	Ln (0.364, 0.358)
Saturated Hydraulic Conductivity	Ksat [m s^{-1}]		Ln (−11.055, 0.37)	Ln (−13.357, 0.37)	1xe-8
Initial hydrological condition:					
Water table height [e]	DWT [%]	U (50,100)			
Rainfall properties:					
Rain intensity	I [m h^{-1}]	U (0 0.2)			
Rain duration	D [h]	Ud (1 72)			
Urban properties:					
Cut slope angle [f]	β [degrees]	N (65.2, 12.6)			
Roof gutters [g]	–	Ud (01)			
Septic tank and Pipe leak [h]	Qt/p [m^3 s^{-1}]	Ud (0 1)			
Urban density	U_d [%]	Ud (0,100)			
Vegetation on urban hillslopes [i]	–	Ud (0 1)			

There are 32 input factors, considering that soil properties are independently sampled for the three soil layers considered.
U = Uniform distribution; Ud = Discrete uniform; N = Normal distribution; Ln = Log-normal distribution.
VG: Van Genuchten parameters for defining suction moisture characteristics curve.
* Layer 1: Residual Soil, Weathering Grade V-VI; Layer2: Weathered material Grade III–IV; Layer3: bedrock Grade I–II; Weathering grades defined according to GEO (1988).
[a] Effective cohesion >0. Effective cohesion c (layer 3) > c (layer 2) > c (layer 1).
[b] Effective friction angle >0. Effective friction angle φ (layer 3) > φ (layer 2) > φ (layer 1). φ < 90°.
[c] γs = γd + 2, where γs is the saturated unit weight. γd (layer 3) > γd (layer 2) > γd (layer 1).
[d] Values from Hodnett and Tomasella (2002) for Sandy Clay Loam material. We impose $n > 1$; θsat > θres; θres >0.
[e] Water table height is defined as a percentage of slope height measured to the toe of the slope.
[f] Slope of the cut forced to be between 39 and 89° and it is always greater than natural slope angle.
[g] Roof gutters on houses. Absent = 0; Present on all houses = 1. Roof type = double pitch (see Fig. 4).
[h] The leak of the septic tank is equal to the leak of the pipe. Absent = 0; Leak from both pipe and tank present = 1 (see Fig. 4).
[i] Vegetation on urban hillslopes to quantify its benefit for landslide mitigation. Absent = 0; Present = 1 (on space left unbuilt – see Fig. 4).

properties are described by 32 input factors, which were all varied according to their probability distribution (Table 1). The vegetation properties (defined in Table 2) were kept fixed (e.g., root depth always 1 m), whereas urban properties were treated as random variables (bottom of Table 1) in accordance with the analysis performed by Bozzolan et al. (2020). The soil properties are described for the three soil layers considered: weathered residual soils and colluvium overlying decomposed rock and volcanic bedrock (as typical in the study site, see section 2).

In the supplementary material section 2, we describe how we obtained the parameters of the probability distributions. Here, we just delineate how the range of variability of current and future rainfalls are treated, which can be of interest for those analyses that include climate-related uncertainty.

Rainfall properties are specified in terms of rainfall intensity and duration. Their ranges of variability were based on intensity-duration-frequency (IDF) relationships derived for the design of the Roseau Dam in Saint Lucia (Klohn-Crippen, 1995). From these IDF curves (represented by the blue lines in Fig. 3), we derived a minimum and maximum rainfall intensity and duration (with maximum respectively 200 mm h^{-1} and 72 h). As suggested by Almeida et al., 2017, we sampled from these ranges independently and uniformly (no a priori knowledge). Under such an assumption we generated a wide range of rainfall intensity-duration combinations that should capture both rainstorms that might have been observed in the past (light-grey area under the IDF curves in Fig. 3) and rainstorms that might be observed in the future (dark-grey area above the IDF curves in Fig. 3).

We could then pick from this wide range of rainfall drivers those rainfall intensity-duration combinations of interest (which might correspond to past events, design/planning requirements, or to different future climate scenarios) and evaluate the corresponding landslide susceptibility.

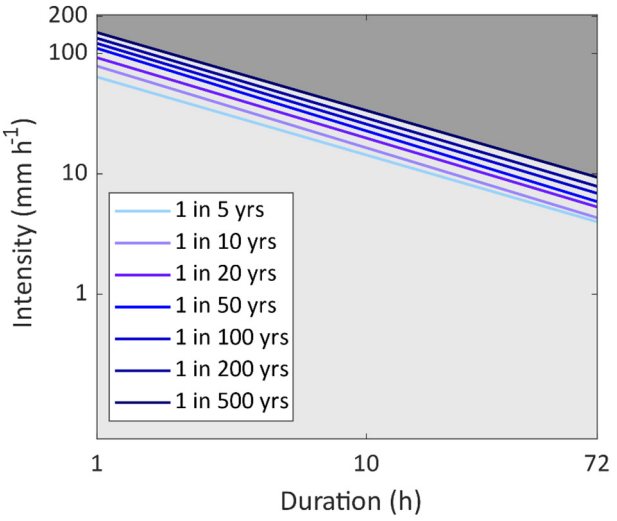

Fig. 3. Rainfall intensity–duration–frequency (IDF) curves for Saint Lucia developed by Klohn-Crippen (1995) using Gumbel analysis of 40 years of daily rainfall data from 15 rainfall gauges across Saint Lucia. Future climate change may increase the frequency of storms and the position of these lines, but such change is still highly uncertain. We thus generated synthetic rainstorm events with rainfall intensity-duration values randomly sampled within the whole grey area, where the light grey area includes rainfall events from observed data (below IDF curves) and the dark grey area (above IDF curves) represents combinations of rainfall intensity-duration not recorded before 1995 but have occurred in the recent past or might occur in the future.

3.3. Generation of libraries of slope stability responses

We used a random uniform approach to randomly sample combinations of input factors from their probability distributions (defined in Table 1). Each combination defines a synthetic hillslope (Fig. 4 is an example for the land cover urban). By repeating the sampling for each land cover, we generated four libraries of synthetic hillslopes (forest, shrub, bare and urban – 30,000 synthetic hillslopes per library with 120,000 synthetic hillslopes in total – Step 2, Fig. 1). Due to the randomness of the sampling, we explicitly checked that combinations of factors were realistic; if not, they were discarded and replaced by another randomly generated, feasible combination. The criteria for these 'feasibility' checks are reported in the footnote of Table 1 (letters a–f).

Table 2
Parameters defining the vegetation properties of trees (land cover: forest) and shrub. Trees properties were used in both land cover 'urban' (as in Fig. 4) and land cover 'forest'. The values are taken from Holcombe et al., (2016) (online Supplement, Table S5). Some modifications were made according to the literature.

Parameter		Unit	Value	
Tree canopy parameters:				
Max leaf storage		mm	5	
Wet canopy evaporation		$ms^{-1} \times 10^{-7}$	2	
Leaf-drip rate		%	0.8	
Stem portion		%	0.0012	
Max trunk storage		Mm	0	
Atmospheric parameter:				
Net radiation		Wm^{-2}	700	
Average daily temperature		Degrees	30	
Average daily rel. humidity		sm^{-1}	0.7	
Canopy resistance		sm^{-1}	70	
Soil aerodynamic resistance		sm^{-1}	50	
Veg. aerodynamic resistance		sm^{-1}	40	
Pressure head sink terms	Oxygen deficiency	M	−0.1	
	Constant	M	−0.35	
	Constant	M	−5	
	Wilting point	M	−14	
Tree/grass parameters:			Trees	Shrub
Surcharge		kNm^{-2}	2	0.3
Leaf area index		mm^{-2}	10	5.8
Canopy cover		%	0.8	0.4
Rooting depth		M	4	1
Max transpiration		$ms^{-1} \times 10^{-7}$	2	1
Root tensile strength		MPa	50	32
Root area ratio		m^2m^{-2}	0.002	0.002

The stability of each hillslope was assessed in CHASM (Combined Hydrology and Stability Model). CHASM is a 2-D mechanistic model which analyses dynamic slope hydrology and its effect on slope stability over time (Anderson, 1990; Anderson and Lloyd, 1991, Wilkinson et al., 2002a, 2002b). The cross section of a slope is represented as a regular mesh of cells (with 1 m resolution in this analysis, as in Fig. 4). Hydrological and geotechnical parameters are specified per each cell, while the initial hydrological conditions define the depth of the water table (DWT) and the matric suction of the top cell of each column.

The dynamic forcing is rainfall, specified in terms of intensity and duration. For each computational time step for the hydrology (here 60 s), a forward explicit finite-difference method is used to solve the Richard's (1-D, vertical flow) and Darcy's (2-D flow) equations, controlling the unsaturated and saturated groundwater flow, respectively. At the end of each simulation hour, the resulting soil pore water pressures (positive and negative) are used as input for the slope stability analysis, which implements Bishop's simplified circular limit equilibrium method (Bishop, 1955). Amongst all possible slip surfaces (centred on a user-defined grid - Fig. 4), an automated search algorithm identifies the one producing minimum *FoS*, which is given as output.

CHASM can represent cut slopes, house loading, and vegetation. In particular, vegetation is represented through rainfall interception, evapotranspiration, root water uptake, vegetation surcharge, and increased permeability and soil cohesion due to the root network (see Wilkinson et al., 2002b). The new extended version CHASM+ (Bozzolan et al., 2020) also includes surface urban water management, through the representation of roof gutters on houses, leaking superficial pipes and buried septic tanks.

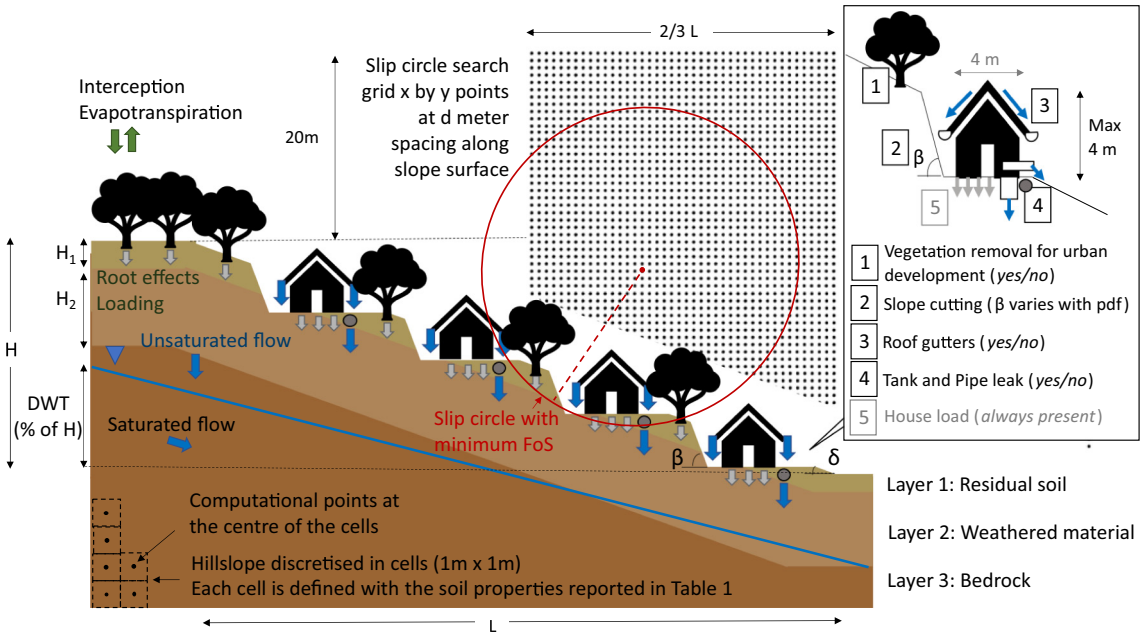

Fig. 4. Example of an urbanised synthetic hillslope generated by randomly sampling from the probability distributions of the input factors specified in Table 1. The hillslope shown in the figure is part of the library representative of the land cover 'urban'. For this reason, not only the geometrical, soil initial boundary conditions and rainfall properties were varied, but also the urban properties (reported at the bottom of Table 1 and represented in the box on the right-hand side of the figure) were considered in the sampling. Under land covers 'forest' and 'shrub', synthetic hillslopes were conceived as fully covered by respectively deep- and shallow-rooted vegetation, while in the 'urban' land cover, trees were inserted in between cuts as shows in the figure. All hillslopes of all landcovers were discretised using a cell size of 1 m × 1 m, and the computational time step for the hydrology was 60 s. The position and size of the slip circle search grid was defined depending on the slope height (H) and length (L) as shown.

Given the large number of simulations, CHASM was run using high performance computers at the University of Bristol – the BlueCrystal Phase 3 which contains 16 × 2.6 GHz Sandy Bridge cores; and Catalyst, an ARM (Advanced RISC Machines) based system which contains 64 cores and 256 GBytes of RAM in each node and runs at 2.2 GHz. Once the simulations were completed, we classified each synthetic hillslope as unstable and stable according to the minimum *FoS* (respectively below and above unity). If the hillslope was predicted as unstable prior to the initiation of the rainfall event (see the Supplementary material, section 2), then it was excluded in the landslide susceptibility assessment because it would represent an unconditionally unstable hillslope (for example, a random combination of steep slope angle with deep soil). However, we used these discarded simulations to assess the maximum soil depths (and therefore soil weight) that hillslopes with certain slope angles could bear before being predicted as unconditionally unstable. Specifically, we defined a 'soil thickness-slope angle threshold' over which hillslopes cannot exist, at least according to CHASM. This threshold was used to facilitate the mapping of the CHASM's slope stability predictions into SUs, as it will be shown in the results section.

3.4. Identification of dominant input factors

In this step we quantified the relative impact of hillslopes, urban and rainfall properties on the slope stability response and identified those that 'dominate' the landslide prediction (Step 4, Fig. 1). We performed this step with a methodology called Global Sensitivity Analysis (Saltelli et al., 2008) that quantifies how the variations in a model's outputs can be attributed to the variations in input factors. Since in our case the model output was binary, as simulated slopes were categorised as unstable (if $FoS < 1$) or stable ($FoS \geq 1$), we used the regional sensitivity analysis (RSA) approach (Hornberger and Spear, 1981), which is particularly suitable when dealing with categorical outputs (but other GSA methods could be used in different applications – for a review see Iooss and Lemaître, 2015). In the RSA approach, the cumulative marginal distribution of each input factor is computed for each output category, i.e., the stable slopes and the unstable ones. If the distributions significantly separate out, we infer that the model output (slope stability) is significantly affected by variations in the considered input factor. The level of separation between the cumulative distributions can be formally measured with the Kolmogorov–Smirnov (KS) statistic and used as a sensitivity index (Pianosi et al., 2016). The confidence intervals of the sensitivity indices can be estimated via a bootstrap technique (Efron and Tibshirani, 1994). The bootstrap randomly draws *Z* samples (with replacement) from the available data to compute *Z* KS statistics for each input factor. The magnitude of fluctuations in the KS statistic from one sample to another represents the level of confidence in the estimation of the sensitivity indices. For this application, we used the SAFE (Sensitivity Analysis For Everybody) toolbox (Pianosi et al., 2015) to perform RSA and to calculate the sensitivity indices and their confidence intervals by the bootstrap technique.

3.5. Assign dominant input factors to Slope Units and calculate their Failure Rates under changing rainfall and land cover conditions

The RSA identified the dominant input factors, i.e. those input factors that contribute the most to determine whether a slope was predicted as stable ($FoS \geq 1$) or unstable ($FoS < 1$). In the next step, we assign each SU with a single value of these dominant factors in order to be able to link each SU with its most similar 2D cross-sectional hillslopes simulated by CHASM. In general, the way to carry out this step depends on the input factors that are found to be dominant and the available data to determine the value of those factors for each SU.

Usually, dominant factors corresponding to geometrical properties can be inferred from a DEM, which are globally available (even if at different resolutions across the globe). In this analysis for example, slope angle was identified as a dominant input factor, so we assigned each SU with a slope angle value equal to the 90th percentile of all the slope angles extrapolated from the DEM for that SU. We then used these slope angles to derive the corresponding soil thickness for each SU. We did this by using a mechanistic-based 'slope angle-soil thickness' relationship derived with our simulation results (as we will explain in the results section and supplementary material).

Soil properties are the most difficult to determine because their estimation is inheritably uncertain over large areas. If available, field and lab data supported by regional geological map and topographical information (e.g. Salciarini et al., 2006) could be used to assign each SU with soil properties estimates. Here, we did not follow this approach as the soil maps for Saint Lucia, in common with most soil maps, do not contain sufficient geotechnical information for stability analysis. Given the lack of reliable information about spatial patterns of the required soil properties, we simply assigned all SUs with the median of the soil properties across the entire island.

Once each SU is defined by its dominant soil and geometrical factors, we can choose a combination of rainstorm and land cover conditions, and look for all the synthetic hillslopes in the simulation library that represent that SU. First, based on the chosen land cover, the library of synthetic hillslopes associated with that particular land cover are retrieved. Then, a search is conducted within that library for the hillslopes with the most similar geometrical, soil and climate properties. Fig. 5 shows how this search is performed. A SU that is, for example, defined by three dominant input factors (X, Y, and Z in the figure) identifies a point (blue dot) in the 3D variability space of the simulated slope stability responses (grey and black dots represent the predicted stable and unstable synthetic simulations respectively). A cubic window centred in that point (red cube in Fig. 5) contains N simulations with hillslopes properties and drivers similar to that SU. If N is equal or greater than a fixed quantity (here, $N \geq 30$), the FR of the SU is calculated as the ratio between the hillslopes predicted as unstable M over N (unstable and stable), otherwise the size of the window is increased until N is reached. By repeating this process for all SUs, we obtained a susceptibility map conditioned by the rainstorm and land cover scenario considered. If we then, for example, wanted to increase the rainstorm intensity, we moved the window in Fig. 5 up along the Z axis and a new FR was re-assessed for all SUs without the need to re-run the model. The same concept applies if a new soil dataset becomes available. In this case, the search would change according to the updated SU properties, making this methodology highly adaptable to changes of the input conditions.

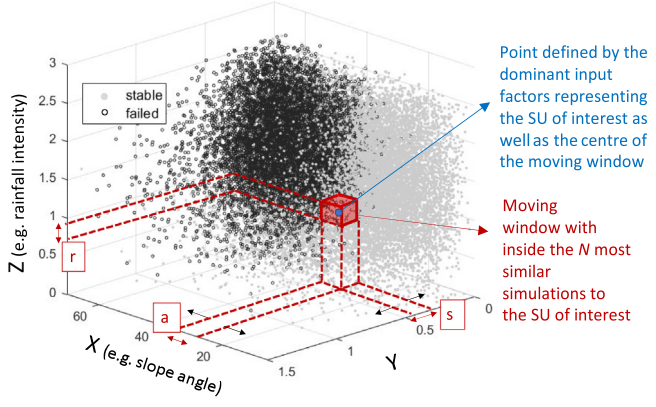

Fig. 5. Representation of the window (red cube) used to calculate the failure rate of the SUs by retrieving the most similar synthetic hillslopes across the variability space. The variables varying along the axis (X, Y, Z) represent the dominant input factors found in the GSA (might be more or less than three). The points represent the stable and unstable simulated synthetic hillslopes. The labels (a), (r), (s) represent the ranges of the input factors whose intersection define such window. The initial width and rate of increase of these ranges are chosen heuristically according to the input factor. When the window includes a number of simulations less than N, the rate of increase is used to iteratively widen the ranges (a), (r), and (s) in the direction of the black arrows until N simulations are included in the cube. For example, if we are interested in calculating the failure rate of a slope with angle 30°, the initial window is centred in 30° with an initial width of 2°, thus including simulated slopes with angles between 29° and 31°. If such initial window does not contain N simulations, the range is increased with a rate of 0.5° in each side (e.g., in the first iteration the range will contain angles between 28.5° and 31.5°).

3.6. Evaluation of the quality of landslide susceptibility maps

In order to evaluate our methodology, we generated a landslide susceptibility map under current land cover (Fig. 2A) for a rainfall event with the characteristics of 2010 Hurricane Tomas, and compared it to the inventory of landslides observed after that event (available at http://www.charim-geonode.net/layers/geonode:landslides_2010_2014). The quality of the map will be high if the areas flagged by the model with high Failure rates are the same areas where landslides were observed after the Hurricane. To evaluate the quality of the map, we used two different techniques: the success rate curve and the Receiver Operating Characteristic (ROC) curve (for discussion about these and other techniques, the reader is referred to Frattini et al., 2010). In the success rate curves, the cumulative percentage of the area of the SUs containing observed landslides is plotted against the cumulative percentage of the area of SUs associated with different FR values (from high to low FR). In the ROC curves, the True Positive rate is plotted against the False Positive Rate, where True and False positive rate are defined as in Fig. 6. In both approaches we therefore obtain a curve similar to those reported in Fig. 6. Steep curves are associated with accurate maps, i.e., maps where the SUs predicted with the highest FR also host the majority of the observed landslides. A quantitative measure of the map's performance can then be obtained by calculating the area under both curves: the larger the area the better the map (Hanley and McNeil, 1982).

4. Analysis and results

4.1. Identify the input factors dominating slope stability in Saint Lucia and assign these factors to Slope Units

In this section we analyse the 120,000 outputs generated by CHASM for the four land covers considered: forest, shrub, bare and urban (30,000 simulations each). We performed RSA to identify the input factors dominating slope stability. Specifically, we computed the sensitivity index of each input factor: a high value of the sensitivity index suggests that the variation of that input factor significantly influences the slope stability response (i.e., the predicted FoS) whereas a value close to zero means that factor has negligible influence. Fig. 7 shows that slope stability is insensitive to many input factors and highly sensitive to five, namely slope angle, effective cohesion, thickness of the layer 1 (residual soil), rain duration and rain intensity.

There is no significant difference in sensitivity between land covers, except for the urban case (darkest bars in Fig. 7) where the sensitivity of cohesion of layer 1 (fifth input from the left) increases while the sensitivity of soil thickness of layer 1 (third input) and of rainfall duration decreases. This is consistent with previous findings, where the change in sensitivity was explained by the fact that when hillslopes are urbanised they are more prone to failure even on less susceptible soils and under less severe rainfall (Bozzolan et al., 2020). The stability of urbanised slopes is also significantly influenced by variations of house density. More considerations on this input factor are reported in the supplementary material, section 3.

In the next step, we assigned the five dominant input factors found with the RSA to the SUs in Saint Lucia. We did this based on the information available, as described in Section 3.5:

- Slope angle: we assigned to each SU the 90th percentile of all slope angles extrapolated from the DEM pixels within that SU.
- Soil thickness of layer 1: we did not have data for this property, but empirical evidence suggests the existence of a threshold that limits the maximum soil thickness able to be maintained for a given slope angle (Patton et al., 2018; Catani et al., 2010). We therefore decided to associate each SU with such 'maximum thickness', calculated as a function of the SU slope angle. We used the library of simulated hillslopes to infer this 'slope angle-soil thickness' relationship. Specifically, we identified the synthetic hillslopes predicted to fail before the beginning of the rainfall events (i.e., hillslopes that are inherently unstable) and derived from

	Predicted	
Observed	SU with FR < FTs	SU with FR > FTs
SU without observed LS	True negative (TN)	False positive (FP)
SU with observed LS	False negative (FN)	True positive (TP)

For ROC curve :	
True positive rate	TP / (TP + FN)
False positive rate	FP / (FP + TN)

SU = Slope Unit
LS = Landslides
FR = Failure rate of the SU

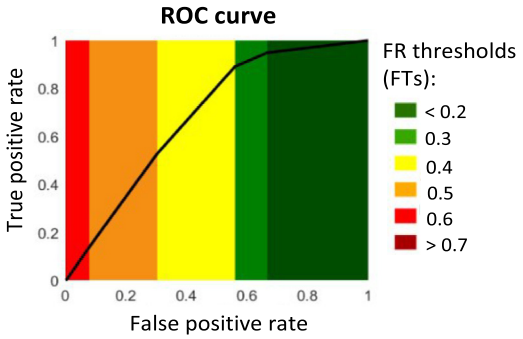

Fig. 6. Accuracy statistics for the calculation of the ROC curve. The *FR* of each SU is compared to different *FR* thresholds (e.g., calculate how many SUs are predicted with *FR* >0.7, 0.6, etc.). We would expect that SUs with predicted *FR* above *high FR* thresholds also contain observed landslides (True Positive) and that SUs with predicted FR below low FR thresholds do not contain observed landslides (True Negative) for the Hurricane Tomas event.

these the maximum thickness sustained at each slope angle value. This method is fully described in the supplementary material, section 4.

- Soil cohesion of layer 1: each SU was assigned with a constant value of 8 kPa, which represents the mode of the probability distribution employed in the stochastic sampling for layer 1 (see Table 1). This is the best available estimate, given the lack of soil cohesion data (inherent at regional scale).

Once each SU was defined with these three input factors, we chose the rainfall conditions of interest (defined by rainfall intensity and duration, which are also two dominant input factors – Fig. 7) and calculated the SUs' *FR* according to the SUs' land cover (assigned from current land cover maps of Fig. 2A or hypothetical) using a moving window as the one described in the methodology Section 3.5 (see also the supplementary material, section 5).

In the next sections, we report the results of two applications. The first represents the susceptibility assessment under rainfall conditions similar to Hurricane Tomas and current land cover (Fig. 2A). In the second application, we generated the susceptibility maps corresponding to hypothetical land covers (expanding deforestation and informal housing) and rainstorm intensities greater than Hurricane Tomas.

4.2. Regional landslide susceptibility for a known rainfall-triggering event

We started by evaluating the landslide susceptibility map corresponding to Hurricane Tomas, which in October 2010 caused severe damage due to flood and landslides throughout Saint Lucia (Van Westen, 2016). The total rainfall was estimated to be 660 mm in some locations, over about a 24 h period, corresponding to a return period between 180 and 200 years depending on the source (van Westen, 2016; Mott MacDonald, 2013). To build the corresponding landslide susceptibility map, we retrieved per each SU the ensemble of (about 30) simulations that have similar slope angle, soil thickness, soil cohesion to that SU and similar rainfall intensity and duration to the Hurricane (as described in Section 3.5). Specifically, we considered a cube (see Fig. 5) with precipitation intensity centred on 28 mm h^{-1} (i.e. 660 mm over 24 h) and duration on 24 h (the range of variation is defined in the supplementary information, section 5). Results are shown in Fig. 8A, together with the locations of 714 real landslides recorded after the hurricane (we considered only the landslides fully contained within the SUs). The quality of the map is evaluated by calculating the area under the curve (*AUC*) of success rate (Fig. 8B) and under the ROC curve (Fig. 8C) (see Section 3.6). These areas are $AUC_{SR} = 0.66$ and $AUC_{ROC} = 0.69$ respectively. Both values indicate an acceptable performance as they fall between 0.5 (the area of a 'random' model that would randomly assign high and low FR values to the SUs containing landslide observations) and 1 (the area of an 'exact' model that would identify high FRs only in those SUs containing landslide observations).

4.3. Regional landslide susceptibility under hypothetical climate and land cover change

We then explored the effects of land cover and climate change on landslide susceptibility by considering five hypothetical scenarios. Scenarios

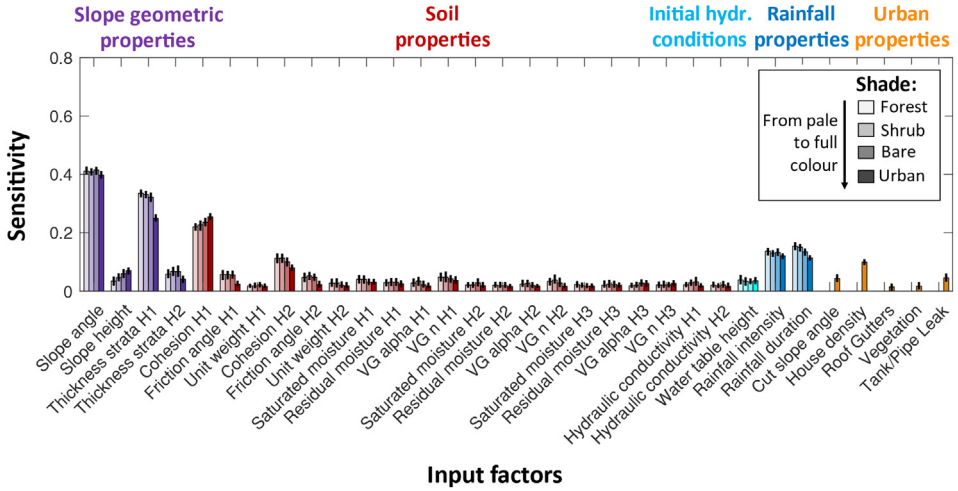

Fig. 7. Sensitivity index of each input factor in the four land cover scenarios. The bars correspond to the mean value of sensitivity for each input factor calculated with bootstrapping, while the black vertical lines at the top of the bars represent the confidence interval (Number of bootstrap resampling Z = 100; significance level for the confidence intervals 0.05).

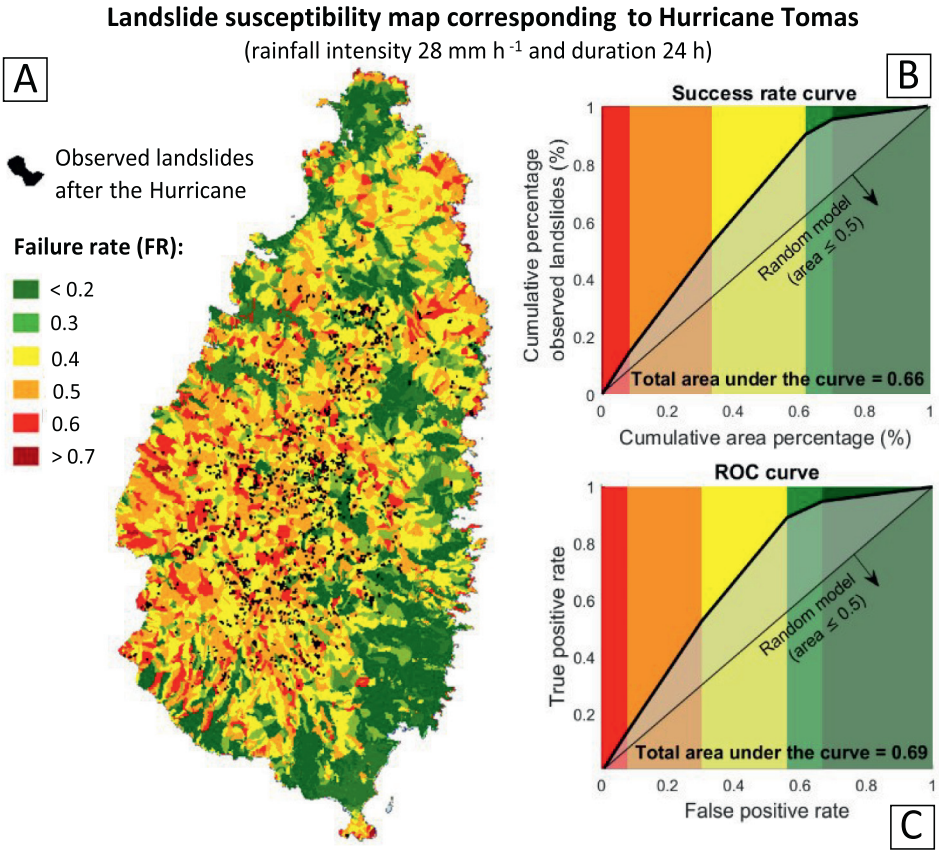

Fig. 8. (A) Landslide susceptibility map associated with a rainstorm event similar to Hurricane Tomas in 2010. The black polygons represent the landslides recorded after the event. The quality of the map is quantified with (B) the success rate curve and (C) the ROC curve.

(A) and (B) are associated to a rainstorm event comparable to Hurricane Tomas but with expanding informal urbanisation (A) and deforestation (B) in all the SUs with angles <50° (i.e. SUs that might be hypothetically urbanised in the future). Scenario (C) uses current land cover conditions but forced by a rainstorm event 10 % more severe than Hurricane Tomas (i.e., a potential future climate scenario – Knutson et al., 2015). Finally, scenarios (A + C) and (B + C) use a combination of the previous land cover and climate change. Fig. 9 shows the resulting susceptibility maps. The arrows report the increase in the number of SUs associated with a *FR* >0.5 (defined as 'hazardous' SUs). In general, the number of hazardous SUs increases in all scenarios. However, the greatest increase occurs when both climate and land cover change are included (about +30 % and + 40 %), with a disproportionate increase in the number of hazardous SUs compared to the scenarios where these two environmental changes are considered independently. For example, the scenarios with only deforestation (B) and only climate change (C) lead respectively to a + 6.4 % and + 5.6 % increase in hazardous SUs, while their combined effect (B + C) lead to an increase of +39 %, which is 4 times the sum of its parts.

5. Discussion

Our Global Sensitivity Analysis (Fig. 7) shows that for all the land covers considered, there are five dominant landslide drivers: slope angle, thickness and cohesion of material layer 1 (i.e., the top strata comprising colluvial and residual soil) and rainfall intensity and duration. The fact that a single model output (the Factor of Safety in our case) is largely controlled by a relatively small number of input factors is not surprising as this almost always is the case when applying GSA to earth system models (Wagener and Pianosi, 2019). The fact that these five factors in particular are dominant is also reasonable, as in general, the steeper the hillslope, and the heavier and weaker the material it's made from, the more unstable it will be; more rainfall penetrating the soil instead decreases soil strength and thus its stability. The relevance of these factors for slope stability is in fact widely recognised (e.g., Guzzetti et al., 2006; Melchiorre and Frattini, 2012; Salciarini et al., 2006; van Westen et al., 2006), but the GSA we performed helpfully quantifies their relative influence on slope stability. In particular, Fig. 7 shows that variations of the geometrical and soil properties influence slope stability more than variations of the rainfall properties in Saint Lucia, regardless of the land cover considered. These results are confirmed also by other studies (Almeida et al., 2017; Folberth et al., 2016; Parker et al., 2016; Samia et al., 2017) and suggest that climate change might have a smaller influence on landslide rates than the intrinsic hillslope properties and their evolution, such as slope topography, lithology, or soil mantle formation and modification due to previous failures. The fact that soil properties have the highest sensitivity indices also suggest that improving the quality of soil databases and better predict soil thickness and soil cohesion across landscapes (Catani et al., 2010; Patton et al., 2018; Dietrich et al., 1995) should be prioritised to improve the accuracy of landslide susceptibility maps (Medina et al., 2021).

Fig. 8 shows that the landslide susceptibility map generated with rainstorm conditions similar to the Hurricane Tomas (Fig. 8) via a comparison to the landslides recorded after that event, gave satisfactory results, with an area under the ROC curve comparable to other similar slope stability analyse that use mechanistic models (Raia et al., 2014; Frattini et al., 2010). Results could be further improved by using a more accurate representation of the precipitation hyetograph (here uniform across the 24 h) (Arnone et al., 2016) or by new datasets, as soon as they become available. For example, if fieldwork in a certain location provides more accurate information about local soil properties, the *FR* of the SUs representing that location could be changed by simply searching for those simulations associated with the updated soil information (without re-running the slope stability model). Given that the initial water table is stochastically varied, the impact of antecedent

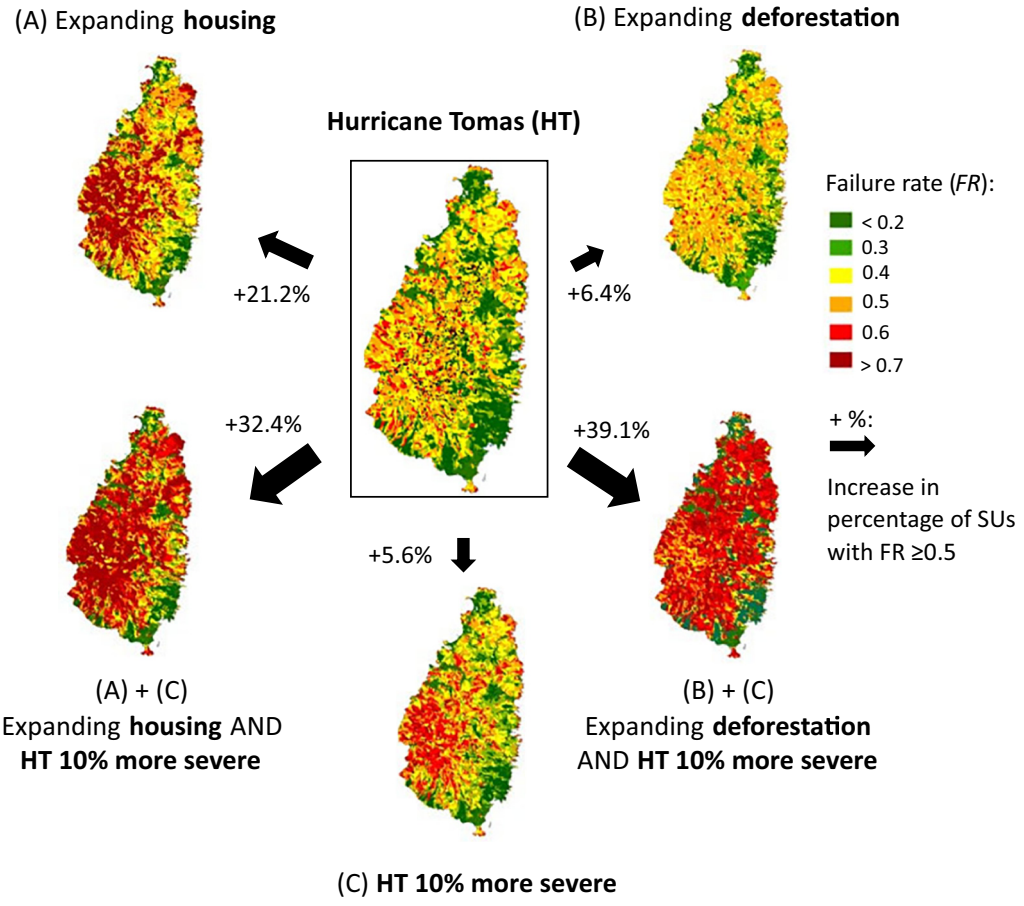

Fig. 9. Ensemble of landslide susceptibility maps forced by different urban and climate scenarios. The framed map is the same reported in Fig. 8 while the other maps represent the susceptibility under the hypothetical scenarios described in Section 4.3. In all maps, each SU has the same slope angle, soil depth and soil cohesion whereas the rainfall intensity and duration and/or the land cover change from one map to the other. These changes define different ensemble of simulations and therefore different FRs. Note that our analysis did not account for planning restrictions such as those preventing deforestation and development in National Forest Reserves.

rainfall on stability could also be analysed by retrieving those simulations with higher (or lower) initial water tables. Additionally, if a given rainfall duration/intensity is associated with a known return period we could associate the same return period to the corresponding susceptibility map, as a function of the remaining input factors.

Fig. 9 shows a quantitative comparison between the landslide susceptibility maps under hypothetical scenarios of expanding informal urbanisation/deforestation (which is plausible as a consequence of the growing urban population in the island – UN-Habitat, 2022), increasing rainstorm severity (potentially representing future climate change) and a scenario where these changes are combined. Three main conclusions can be drawn. First, *FR* generally increases when SUs pass from vegetated to bare or urbanised land cover, which is compatible with previous empirical and statistical analyses (Reichenbach et al., 2014; Vanacker et al., 2003; Pisano et al., 2017; Persichillo et al., 2018). Plants can increase stability by intercepting rainfall (so by decreasing the pore water pressure within hillslopes) and by strengthening the soil with their root network; unregulated housing can instead make a hillslope more likely to fail by steepening its angles via hill cutting, and by increasing the water infiltrating the soil via poorly managed urban water systems. A second conclusion is that expanding informal housing significantly increases landslide susceptibility under current rainfall conditions (scenario A in Fig. 9) and such an increase is greater than the one obtained when only more severe (yet unobserved) rainfall intensities are considered (scenario C in Fig. 9). That informal urbanisation can enhance landslide activity is empirically well documented (Anderson et al., 2008; Smyth and Royle, 2000; Diaz, 1992) but few studies quantify its influence on slope susceptibility (Holcombe et al., 2016; Bozzolan et al., 2020). In this analysis, we showed how the impact of potential future urbanisation can be compared to the impact of potential climate change. More of these comparisons should be performed to better support targeted landslide mitigation decisions. Finally, Fig. 9 shows that when we combine land cover and climate change scenarios (A + C and B + C), landslide susceptibility disproportionally increases (i.e. "the whole is greater than the sum of its parts"), highlighting the importance of considering both these environmental changes in landslide predictions. A comparison of our results with previous findings is difficult, since only very few investigations have included both vegetation and climate change in landslide susceptibility assessments, while none included informal housing. Hürlimann et al. (2022), for example, found that the stabilising influence of a hypothetical increase in forested area was considerably larger than the destabilising effects related to rainfall changes – assuming that the beneficial effect of root reinforcement on stability dominates over the increase in pore water pressure due to the larger precipitation. In this analysis, we demonstrate that (the lack of) vegetation can have different impacts on stability depending on the rainfall scenario considered (scenario B vs scenario B + C) and that such an impact is not linear with the increase of precipitation severity (scenario B + C).

The susceptibility maps presented in this paper are only examples of how the synthetic library of slope stability responses could be used. Risk reduction consultants, city planners, engineers and those involved in community development could for example explore the catalogue of simulations results to test the effectiveness of landslide mitigation measures by comparing those simulations with or without the intervention (for example, increasing vegetation in hotspot areas for landslide susceptibility) in order to quantify the corresponding decrease in landslide failure rates (as suggested in Ozturk et al., 2022). Another application could include the

construction of rainfall thresholds for triggering landslides for different hillslopes angles (e.g. a threshold for the steepest and shallowest part of a catchment) or different land covers (as natural vs urban in Bozzolan et al., 2020). By adapting the input parameters and forcing scenarios, the suggested methodological approach enables the type of analysis advocated by Galasso et al. (2021) "*in which different development scenarios and detailed urban design and policy options can be considered, evaluated, modified and rated by a range of stakeholders*". Importantly, the modelling includes the uncertainty of both urban and rainfall drivers as well as of the hydrological and geotechnical properties of the hillslopes: if the assessed range of slopes/scenarios is found to be stable over and above these uncertainties, the confidence in the model's predictions increases. This type of quantitative information is particularly relevant in the Tropics, where urban growth and rainfall-triggered landslides have the potential to significantly increase in the future (Tabari, 2020; UN, 2019; Ozturk et al., 2022), but where the data scarcity and limited economic capacity is tackling landslide risk awareness and mitigation. Similar applications might become useful mainly for small islands like the Caribbean, where it is often difficult to obtain land cover change information or future rainfall projections due to the limited data sources (Seneviratne et al., 2012).

Given that the generated synthetic library of slope stability responses may be relevant for all other type of analyses suggested above as well as for other locations with similar natural, climate and urban characteristics, we rendered it available for download at the University of Bristol data repository https://doi.org/10.5523/bris.2fy9l5xd3f112sf9e6nt8cv8n (Bozzolan et al., 2022).

5.1. Limitations

All of the results presented here are subject to the limitation of the input data and the assumptions made in this study. However, utilisation of Global Sensitivity Analysis as part of our modelling strategy enables us to test the influence of assumptions and choices on the input factors (such as soil and rainfall parameters) even in the context of climate change impact studies where we cannot rely on a comparison with observations of the impact we analyse (Wagener et al., 2022). Using different probability distributions for the stochastic sampling of CHASM input factors might lead to identifying different influential factors through global sensitivity analysis (Paleari and Confalonieri, 2016). The computation time and the level of skills required to run stochastically mechanistic-based models might represent a limitation. However, cloud computing gets around the first problem, whereas shared datasets of simulations results (such as the one we provide) widens the access to these type of analyses also to less expert users (Ozturk et al., 2022). Vegetation is represented in a simplistic way (although the physical representation of vegetation in CHASM is relatively sophisticated) as only two types (forest and shrub) are simulated and the effect of variations of their physical features on slope stability is not analysed. Vegetation properties might change with climate (Dixon and Brook, 2007; Collison et al., 2000), but in this analysis they are considered independent. We assigned the same cohesion value to all the SUs (specifically, we used the mode of the distribution of values obtained from measurements in different locations of the region) in the absence of further data to enable allocation of different values to different SUs. However, soil composition and strength vary from one location to another, even within homogeneous layers (Burton et al., 1998). The large uncertainty associated with the spatial distribution of soil cohesion and soil thickness is common for this type of analyses (Salciarini et al., 2006; Melchiorre and Frattini, 2012). Yet, the impact of this uncertainty may be reduced in this analysis, given that we use our methodology not to predict in absolute values landslide probability but to gain insights on the relative change of landslide occurrence between different scenarios – a piece of information that is often sufficient to inform environmental planning (Van Beek and Van Asch, 2004). Furthermore, as previously noted, our approach allows for individual SUs to be re-assessed as new data is obtained, or if hillslope-specific assessment is required for determining site-specific stability behaviours and mitigation measures.

6. Conclusions

In this paper we propose a new methodology to generate national-scale landslide susceptibility maps under a wide range of combinations of current or hypothetical urban expansion scenarios and climate change drivers. We test our approach for the island of Saint Lucia, which is representative of data scarce and landslide-prone regions in the humid tropics. These results are unique as, for the first time, they include informal urbanisation and climate change in a regional (in our case 617 km^2) susceptibility assessment, while also considering the influence of the model parameters uncertainty.

For the case study of Saint Lucia, we can summarise our main findings as follows:

1) Geometrical (slope angle and the thickness of the first layer of residual soil) and soil properties are the predisposing factors that most dominate the slope stability response – their influence is greater than rainfall, at least at this island-wide scale.
2) The susceptibility map generated under rainfall conditions similar to Hurricane Tomas identifies the location of the landslides triggered by that rainstorm event with reasonable accuracy.
3) Expanding informal housing increases landslide susceptibility more than hypothetical climate change scenarios. Furthermore, the joint effect of land cover and climate change increases landslide susceptibility disproportionally, i.e. more than the sum of the two scenarios considered independently.

Our method offers two main advantages compared to other methods currently in use. First, it detects the dominant slope stability drivers and quantifies their relative importance. Such information can help stakeholders to assess where investments should be prioritised to attempt to reduce uncertainty in slope stability predictions. Second, it is capable of dealing with non-stationary conditions and so it can be updated as frequently as required, just by picking the most relevant modelled scenarios. Such flexibility also allows the quantification of the relative and joint impact of a wide range of hypothetical scenarios on regional landslide predictions. This information could better support national climate adaptation planning and landslide risk reduction investments in data-scarce developing countries.

CRediT authorship contribution statement

Elisa Bozzolan: Conceptualization, Formal analysis, Investigation, Visualization, Writing – original draft, Writing – review & editing.

Elizabeth Holcombe: Conceptualization, Writing – review & editing.

Francesca Pianosi: Conceptualization, Visualization, Writing – review & editing.

Thorsten Wagener: Conceptualization, Writing – review & editing.

Massimiliano Alvioli: SU delineation; Writing – review & editing.

Ivan Marchesini: SU delineation; Writing – review & editing.

Data availability

Input data specified in the paper. The resulting synthetic dataset is available at the University of Bristol data repository, data.bris (https://data.bris.ac.uk/data/), at https://doi.org/10.5523/bris.2fy9l5xd3f112sf9e6nt8cv8n.

Declaration of competing interest

The authors declare they have not known competing financial interests or personal relationships that could have appeared to influence the work reported in this paper.

Acknowledgments

The first author was supported by an EPSRC DTP studentship (grant no. EP/N509619/1). Francesca Pianosi is partially funded by the Engineering and Physical Sciences Research Council (EPSRC) "Living with Environmental Uncertainty" Fellowship (EP/R007330/1). Funding for Thorsten

Wagener has been provided by the Alexander von Humboldt Foundation in the framework of the Alexander von Humboldt Professorship endowed by the German Federal Ministry of Education and Research.

Appendix A. Supplementary data

Supplementary data to this article can be found online at https://doi.org/10.1016/j.scitotenv.2022.159412.

References

Almeida, S., Holcombe, E.A., Pianosi, F., Wagener, T., 2017. Dealing with deep uncertainties in landslide modelling for disaster risk reduction under climate change. Nat. Hazards Earth Syst. Sci. 17, 225–241. https://doi.org/10.5194/nhess-17-225-2017.

Alvioli, M., Marchesini, I., Reichenbach, P., Rossi, M., Ardizzone, F., Fiorucci, F., Guzzetti, F., 2016. Automatic delineation of geomorphological slope units with r.slopeunits v1.0 and their optimization for landslide susceptibility modeling. Geosci. Model Dev. 9, 3975–3991. https://doi.org/10.5194/gmd-9-3975-2016.

Alvioli, M., Melillo, M., Guzzetti, F., Rossi, M., Palazzi, E., von Hardenberg, J., Brunetti, M.T., Peruccacci, S., 2018. Implications of climate change on landslide hazard in Central Italy. Sci. Total Environ. 630, 1528–1543. https://doi.org/10.1016/j.scitotenv.2018.02.315.

Alvioli, M., Guzzetti, F., Marchesini, I., 2020. Parameter-free delineation of slope units and terrain subdivision of Italy. Geomorphology 358, 107124. https://doi.org/10.1016/j.geomorph.2020.107124.

Alvioli, M., Marchesini, I., Pokharel, B., Gnyawali, K., Lim, S., 2022. Geomorphological slope units of the Himalayas. J.Maps https://doi.org/10.1080/17445647.2022.2052768.

Anderson, M.G., 1990. A Feasibility Study in Mathematical Modelling of Slope Hydrology and Stability, Report. Geotechnical Control Office Civil Engineering Services Department, Hong Kong.

Anderson, M.G., Holcombe, E.A., 2013. Community-based Landslide Risk Reduction: Managing Disasters in Small Steps. The World Bank.

Anderson, M.G., Lloyd, D.M., 1991. Using a combined slope hydrology-stability model to develop cut slope design charts. Proc. - Inst. Civ. Eng. Part 2. Res. Theory. 91, pp. 705–718. https://doi.org/10.1016/0148-9062(92)90903-d.

Anderson, M., Holcombe, L., Flory, R., Renaud, J.P., 2008. Implementing low-cost landslide risk reduction: a pilot study in unplanned housing areas of the Caribbean. Nat. Hazards 47, 297–315. https://doi.org/10.1007/s11069-008-9220-z.

Arnone, E., Dialynas, Y.G., Noto, L.V., Bras, R.L., 2016. Accounting for soil parameter uncertainty in a physically based and distributed approach for rainfall-triggered landslides. Hydrol. Process. 944, 927–944. https://doi.org/10.1002/hyp.10609.

Bernardie, S., Vandromme, R., Thiery, Y., Houet, T., Grémont, M., Masson, F., Grandjean, G., Bouroullec, I., 2020. Modelling landslide hazard under global change: the case of a Pyrenean valley. Nat. Hazards Earth Syst. Sci., 1–34 https://doi.org/10.5194/nhess-2019-311.

Bishop, A.W., 1955. The Use of the Slip Circle in the Stability Analysis of Slopes. 5, pp. 7–17. https://doi.org/10.1680/geot.1955.5.1.7.

Bozzolan, E., Holcombe, E.A., Pianosi, F., Wagener, T., 2020. Including informal housing in slope stability analysis – an application to a data-scarce location in the humid tropics. Nat. Hazards Earth Syst. Sci. Discuss., 1–20 https://doi.org/10.5194/nhess-2020-207.

Bozzolan, E., Holcombe, E.A., Pianosi, F., Wagener, W., 2022. StLucia_STOTEN2022_simulation_dataset. https://doi.org/10.5523/bris.2fy9l5xd3f112sf9e6nt8cv8n.

Burton, A., Arkell, T.J., Bathurst, J.C., 1998. Field variability of landslide model parameters. Environ. Geol. 35, 100–114. https://doi.org/10.1007/s002540050297.

Carrara, A., Cardinali, M., Detti, R., Guzzetti, F., Pasqui, V., Reichenbach, P., 1991. GIS techniques and statistical models in evaluating landslide hazard. Earth Surf. Process. Landforms 16, 427–445. https://doi.org/10.1002/esp.3290160505.

Carrara, A., Cardinali, M., Guzzetti, F., Reichenbach, P., 1995. Gis Technology in Mapping Landslide Hazard, pp. 135–175 https://doi.org/10.1007/978-94-015-8404-3_8.

Catani, F., Segoni, S., Falorni, G., 2010. An empirical geomorphology-based approach to the spatial prediction of soil thickness at catchment scale. Water Resour. Res. 46, 1–15. https://doi.org/10.1029/2008WR007450.

Collison, A., Wade, S., Griffiths, J., Dehn, M., 2000. Modelling the impact of predicted climate change on landslide frequency and magnitude in SE England. Eng. Geol. 55, 205–218. https://doi.org/10.1016/S0013-7952(99)00121-0.

DeGraff, J.F., 1985. Landslide Hazard on St. Lucia, West Indies, Final Report. Organization of American States, Washington, D. C.

Diaz, V.J., 1992. Landslides in the squatter settlements of Caracas; towards a better understanding of causative factors. Environ. Urban. 4, 80–89.

Dietrich, W.E., Reiss, R., Montgomery, D.R., Hsu, M.-L., 1995. A process-based model for colluvial soil depth and shallow landsliding using digital elevation data. Hydrol. Process. 9, 383–400. https://doi.org/10.1002/hyp.3360090311.

Dixon, N., Brook, E., 2007. Impact of Predicted Climate Change on Landslide Reactivation: Case Study of Mam Tor, UK. 4, pp. 137–147. https://doi.org/10.1007/s10346-006-0071-y.

Efron, B., Tibshirani, R.J., 1994. An Introduction to the Bootstrap. CRC Press.

Folberth, C., Skalský, R., Moltchanova, E., Balkovič, J., Azevedo, L.B., Obersteiner, M., Van Der Velde, M., 2016. Uncertainty in soil data can outweigh climate impact signals in global crop yield simulations. Nat. Commun. 7, 1–13. https://doi.org/10.1038/ncomms11872.

Frattini, P., Crosta, G., Carrara, A., 2010. Techniques for evaluating the performance of landslide susceptibility models. Eng. Geol. 111, 62–72. https://doi.org/10.1016/j.enggeo.2009.12.004.

Galasso, C., McCloskey, J., Pelling, M., Hope, M., Bean, C., Cremen, G., Guragain, R., Hancilar, U., Menoscal, J., Mwang'a, K., Phillips, J., Rush, D., Sinclair, H., 2021. Editorial. Risk-based, pro-poor urban design and planning for tomorrow's Cities. Int. J. Disaster Risk Reduct., 102158 https://doi.org/10.1016/j.ijdrr.2021.102158.

Gariano, S.L., Guzzetti, F., 2016. Landslides in a changing climate. Earth-Sci.Rev. 162, 227–252. https://doi.org/10.1016/j.earscirev.2016.08.011.

Gariano, S.L., Petrucci, O., Guzzetti, F., 2015. Changes in the occurrence of rainfall-induced landslides in Calabria, southern Italy, in the 20th century. Nat. Hazards Earth Syst. Sci. 15, 2313–2330. https://doi.org/10.5194/nhess-15-2313-2015.

GEO, 1988. Geoguide 3- Guide to Rock and Soil Descriptions. 177. Geotech. Eng. Off.

Glade, T., 2003. Landslide Occurrence as a Response to Land Use Change: A Review of Evidence From New Zealand. 51, pp. 297–314. https://doi.org/10.1016/S0341-8162(02)00170-4.

Guzzetti, F., Carrara, A., Cardinali, M., Reichenbach, P., 1999. Landslide Hazard Evaluation: A Review of Current Techniques and Their Application in a Multi-scale Study, Central Italy. 31, pp. 181–216. https://doi.org/10.1016/S0169-555X(99)00078-1.

Guzzetti, F., Reichenbach, P., Ardizzone, F., Cardinali, M., Galli, M., 2006. Estimating the Quality of Landslide Susceptibility Models. 81, pp. 166–184. https://doi.org/10.1016/j.geomorph.2006.04.007.

Hanley, J.A., McNeil, B.J., 1982. The meaning and use of the area under a receiver operating characteristic (ROC) curve. Radiology 143, 29–36.

Haque, U., da Silva, P.F., Devoli, G., Pilz, J., Zhao, B., Khaloua, A., Wilopo, W., Andersen, P., Lu, P., Lee, J., Yamamoto, T., Keellings, D., Jian-Hong, W., Glass, G.E., 2019. The human cost of global warming: deadly landslides and their triggers (1995–2014). Sci. Total Environ. 682, 673–684. https://doi.org/10.1016/j.scitotenv.2019.03.415.

Holcombe, E.A., Beesley, M.E.W., Vardanega, P.J., Sorbie, R., 2016. Urbanisation and landslides: hazard drivers and better practices. Proc. Inst. Civ. Eng. - Civ. Eng. 169, 137–144. https://doi.org/10.1680/jcien.15.00044.

Hornberger, G.M., Spear, R.C., 1981. An approach to the preliminary analysis of environmental systems. J. Environ. Manag. 12, 7–18.

Hürlimann, M., Guo, Z., Puig-Polo, C., Medina, V., 2022. Impacts of Future Climate and Land Cover Changes on Landslide Susceptibility: Regional Scale Modelling in the Val d'Aran Region (Pyrenees, Spain). 19, pp. 99–118. https://doi.org/10.1007/s10346-021-01775-6.

Iooss, B., Lemaître, P., 2015. A review on global sensitivity analysis methods. Uncertainty Management in Simulation-optimization of Complex Systems. Springer, pp. 101–122.

Jetten, V., 2016. CHaRIM Project Saint Lucia National Flood Hazard Map Methodology and Validation Report.

Klohn-Crippen, 1995. Roseau Dam and ancillary works. Tropical storm Debbie, final report on hydrology, Unpublished report held by WASCO, Saint Lucia.

Knutson, T.R., Sirutis, J.J., Zhao, M., Tuleya, R.E., Bender, M., Vecchi, G.A., Villarini, G., Chavas, D., 2015. Global projections of intense tropical cyclone activity for the late twenty-first century from dynamical downscaling of CMIP5/RCP4.5 scenarios. J. Clim. 28, 7203–7224. https://doi.org/10.1175/JCLI-D-15-0129.1.

Larsen, M.C., 2008. Rainfall-triggered landslides, anthropogenic hazards, and mitigation strategies. Adv. Geosci. 14, 147–153. https://doi.org/10.5194/adgeo-14-147-2008.

MacDonald, Mott, 2013. Landslide Risk Assessment for Saint Lucia's Primary Road Network, Hurric. Tomas Rehabil. Reconstr. Final Feasibility Rep. 258.

Maes, J., Kervyn, M., de Hontheim, A., Dewitte, O., Jacobs, L., Mertens, K., Vanmaercke, M., Vranken, L., Poesen, J., 2017. Landslide risk reduction measures: a review of practices and challenges for the tropics. Prog. Phys. Geogr. 41, 191–221.

Medina, V., Hürlimann, M., Guo, Z., Lloret, A., Vaunat, J., 2021. Fast physically-based model for rainfall-induced landslide susceptibility assessment at regional scale. Catena 201, 105213. https://doi.org/10.1016/j.catena.2021.105213.

Melchiorre, C., Frattini, P., 2012. Modelling probability of rainfall-induced shallow landslides in a changing climate, Otta, Central Norway. Clim. Chang. 113, 413–436. https://doi.org/10.1007/s10584-011-0325-0.

Migoń, P., 2010. Mass movement and landscape evolution in weathered granite and gneiss terrains. Geol. Soc. Eng. Geol. Spec. Publ. 23, 33–45. https://doi.org/10.1144/EGSP23.4.

Ozturk, U., Bozzolan, E., Holcombe, E.A., Shukla, R., Pianosi, F., Wagener, T., 2022. How climate change and unplanned urban sprawl bring more landslides,Nature. Nature 608 (7922), 262–265 August.

Paleari, L., Confalonieri, R., 2016. Sensitivity analysis of a sensitivity analysis: we are likely overlooking the impact of distributional assumptions. Ecol. Model. 340, 57–63. https://doi.org/10.1016/j.ecolmodel.2016.09.008.

Parker, R.N., Hales, T.C., Mudd, S.M., Grieve, S.W.D., Constantine, J.A., 2016. Colluvium supply in humid regions limits the frequency of storm-triggered landslides. Sci. Rep. 6, 1–7. https://doi.org/10.1038/srep34438.

Patton, N.R., Lohse, K.A., Godsey, S.E., Crosby, B.T., Seyfried, M.S., 2018. Predicting soil thickness on soil mantled hillslopes. Nat. Commun. 9. https://doi.org/10.1038/s41467-018-05743-y.

Persichillo, M.G., Bordoni, M., Cavalli, M., Crema, S., Meisina, C., 2018. The Role of Human Activities on Sediment Connectivity of Shallow Landslides. 160, pp. 261–274. https://doi.org/10.1016/j.catena.2017.09.025.

Pianosi, F., Sarrazin, F., Wagener, T., 2015. A matlab toolbox for global sensitivity analysis. Environ. Model. Softw. 70, 80–85. https://doi.org/10.1016/j.envsoft.2015.04.009.

Pianosi, F., Beven, K., Freer, J., Hall, J.W., Rougier, J., Stephenson, D.B., Wagener, T., 2016. Sensitivity analysis of environmental models: a systematic review with practical workflow. Environ. Model. Softw. 79, 214–232. https://doi.org/10.1016/j.envsoft.2016.02.008.

Pisano, L., Zumpano, V., Malek, Rosskopf, C.M., Parise, M., 2017. Variations in the susceptibility to landslides, as a consequence of land cover changes: a look to the past, and another towards the future. Sci. Total Environ. 601–602, 1147–1159. https://doi.org/10.1016/j.scitotenv.2017.05.231.

Raia, S., Alvioli, M., Rossi, M., Baum, R.L., Godt, J.W., Guzzetti, F., 2014. Improving predictive power of physically based rainfall-induced shallow landslide models: a probabilistic approach. Geosci. Model Dev. 7, 495–514. https://doi.org/10.5194/gmd-7-495-2014.

Reichenbach, P., Busca, C., Mondini, A.C., Rossi, M., 2014. The influence of land use change on landslide susceptibility zonation: the Briga Catchment Test Site (Messina, Italy). Environ. Manag. 54, 1372–1384. https://doi.org/10.1007/s00267-014-0357-0.

Reichenbach, P., Rossi, M., Malamud, B.D., Mihir, M., Guzzetti, F., 2018. A review of statistically-based landslide susceptibility models. Earth-Sci.Rev. 180, 60–91. https://doi.org/10.1016/j.earscirev.2018.03.001.

Salciarini, D., Godt, J.W., Savage, W.Z., Conversini, P., Baum, R.L., Michael, J.A., 2006. Modeling Regional Initiation of Rainfall-induced Shallow Landslides in the Eastern Umbria Region of Central Italy. 3, pp. 181–194. https://doi.org/10.1007/s10346-006-0037-0.

Saltelli, A., Ratto, M., Andres, T., Campolongo, F., Cariboni, J., Gatelli, D., Saisana, M., Tarantola, S., 2008. Global Sensitivity Analysis: The Primer. John Wiley & Sons.

Samia, J., Temme, A., Bregt, A., Wallinga, J., Guzzetti, F., Ardizzone, F., Rossi, M., 2017. Do landslides follow landslides?Insights in path dependency from a multi-temporal landslide inventory. 14, pp. 547–558. https://doi.org/10.1007/s10346-016-0739-x.

Seneviratne, S., Nicholls, N., Easterling, D., Goodess, C., Kanae, S., Kossin, J., Luo, Y., Marengo, J., McInnes, K., Rahimi, M., et al., 2012. Changes in Climate Extremes and Their Impacts on the Natural Physical Environment: An Overview of the IPCC SREX Report.

Smyth, C.G., Royle, S.A., 2000. Urban landslide hazards: incidence and causative factors in Niteroi, Rio de Janeiro state, Brazil. Appl. Geogr. 20, 95–118. https://doi.org/10.1016/S0143-6228(00)00004-7.

Tabari, H., 2020. Climate change impact on flood and extreme precipitation increases with water availability. Sci. Rep. 10, 1–10. https://doi.org/10.1038/s41598-020-70816-2.

UN, 2019. World Urbanization Prospects: The 2018 Revision, Online Edition (ST/ESA/SER.A/420). United Nations, Department of Economic and Social Affairs, Population Division, New York: United Nations 197-236 pp.

UN-Habitat, 2022. World Cities Report 2022. Envisaging the Future of Cities.

Van Beek, L.P.H., Van Asch, T.W.J., 2004. Regional assessment of the effects of land-use change on landslide hazard by means of physically based modelling. Nat. Hazards 31, 289–304. https://doi.org/10.1023/B:NHAZ.0000020267.39691.39.

Vanacker, V., Vanderschaeghe, M., Govers, G., Willems, E., Poesen, J., Deckers, J., De Bievre, B., 2003. Linking Hydrological, Infinite Slope Stability and Land-use Change Models Through GIS for Assessing the Impact of Deforestation on Slope Stability in High Andean Watersheds. 52, pp. 299–315. https://doi.org/10.1016/S0169-555X(02)00263-5.

Wagener, T., Pianosi, F., 2019. What has Global Sensitivity Analysis ever done for us? A systematic review to support scientific advancement and to inform policy-making in earth system modelling. Earth-Sci. Rev. 194, 1–18. https://doi.org/10.1016/j.earscirev.2019.04.006.

Wagener, T., Reinecke, R., Pianosi, F., 2022. On the evaluation of climate change impact models. Wiley Interdiscip. Rev. Clim. Chang. e772. https://doi.org/10.1002/wcc.772.

van Westen, C.J., 2016. Caribbean Handbook on Risk Information Management National Scale Landslide Susceptibility Assessment for Saint Lucia.

van Westen, C.J., van Asch, T.W.J., Soeters, R., 2006. Landslide hazard and risk zonation - why is it still so difficult? Bull. Eng. Geol. Environ. 65, 167–184. https://doi.org/10.1007/s10064-005-0023-0.

Wilkinson, P.L., Anderson, M.G., Lloyd, D.M., 2002a. An integrated hydrological model for rain-induced landslide prediction. Earth Surf. Process. Landforms 27, 1285–1297. https://doi.org/10.1002/esp.409.

Wilkinson, P.L., Anderson, M.G., Lloyd, D.M., Renaud, J.P., 2002b. Landslide hazard and bioengineering: towards providing improved decision support through integrated numerical model development. Environ. Model. Softw. 17, 333–344. https://doi.org/10.1016/S1364-8152(01)00078-0.

World Bank, 2012. Disaster Risk Management in Latin America and the Caribbean Region: GFDRR Country Notes (English). World Bank, COPERNICUS GESELLSCHAFT MBH, Washington, D.C 226–235 pp.